Joint 48th IEEE Conference on Decision and Control and
28th Chinese Control Conference
Shanghai, P.R. China, December 16-18, 2009

High Confinement at Low Power Input in Magnetic Fusion Plasmas: Analysis of Trade-offs Using Stability Theory

Rowena Ball
Mathematical Sciences Institute and Research School of Physics & Engineering
The Australian National University, Canberra ACT 0200 Australia
e-mail Rowena.Ball@anu.edu.au
Current address: Defence Science and Technology Organisation, Canberra ACT 2600 Australia

Abstract— **Physics-based conditions are used to unfold trapped or persistent degenerate singularities in a dynamical model for plasma confinement transitions. Structural characterization of the resulting enhanced model achieves unification of previous disparate views of confinement transition physics, provides valuable intelligence on shear flow suppression of turbulence and oscillatory régimes, and suggests targeted experimental design, control and optimization strategies for new-generation fusion experiments. The stability trade-offs involved in achieving high confinement at low power input are discussed.**

I. INTRODUCTION

Magnetic fusion plasmas are strongly driven non-equilibrium systems in which the kinetic energy of small-scale turbulent fluctuations can drive the formation of large-scale, stable, coherent structures such as shear and zonal flows that can function as barriers to or channels for transport. This inherent tendency to self-organise is a striking characteristic of flows where Lagrangean fluid elements experience an effective two-dimensional velocity field, and is believed to be due to two linked and consequential attributes of the ideal two-dimensional flow: a second quadratic conserved quantity, mean square vorticity or enstrophy, which in turn allows significant spectral fluxes of energy to low wavenumbers or large spatial scales [1]. In three dimensions, turbulence is associated with stretching and folding of vorticity, but a two-dimensional flow cannot turn or stretch the vorticity vector. The distinctive properties of quasi two-dimensional fluid motion are the basis of natural phenomena such as zonal and coherent structuring of planetary flows, but are generally under-exploited in technology.

These "inverse cascade" processes endemic to the ideal two-dimensional flow are important in the large scale behaviour of rotating and stratified geophysical flows and in magnetic fusion plasmas. Furthermore, since the dominant motions over two spatial dimensions largely determine how they arrange themselves long-term (the climates) two-dimensional fluid dynamics is an acceptable first approximation. However, the instability mechanisms are essentially three-dimensional. This is the sense in which I use the term "quasi two-dimensional flow" to describe magnetic fusion plasmas.

In such plasmas the most potentially useful effect of quasi two-dimensional fluid motion is suppression of high wavenumber turbulence that generates anomalous cross-field transport fluxes and degrades confinement [2], which can manifest as a dramatic enhancement of sheared poloidal or zonal flows and concomitant reduction in turbulent transport. These low- to high-confinement (L–H) transitions have been the subject of intensive experimental, *in numero,* and theoretical and modelling investigations since the 1980s. Two major strands in the literature emerged early and have persisted: (I) Confinement transitions are an internal, quasi two-dimensional flow phenomenon and occur spontaneously when the rate of upscale transfer of kinetic energy from turbulence to shear and zonal flows, via Reynolds stress decorrelation, exceeds the nonlinear dissipation rate [3]; (II) Confinement transitions are due to a net loss of ions near the plasma edge (because ions have larger larmor radii than electrons), the resulting electric field providing a torque which drives the poloidal shear flow nonlinearly [4], [5], [6].

In this work these different views of the physics of confinement transitions are smoothly reconciled in a unified dynamical model for the the coupled dynamics of potential energy, turbulent kinetic energy, and shear flow kinetic energy subsystems. The model is developed by a stepwise iterative process: 1. Identify and interrogate degenerate (high-order) trapped or persistent singularities in the simplest model; 2. Unfold the singularities in physically meaningful ways; 3. Interrogate any new singularities that occur in enhanced model; 4. Repeat steps 2 and 3 until the model is free of pathological or persistent degenerate singularities (i.e., smooth), self-consistent, and therefore predictive.

In the context of control of fusion plasmas this analysis provides the control engineer with knowledge of where and how to access and optimise improved confinement states given the constraints of minimising the power supplied and avoiding — or perhaps exploiting — regimes of instability, using the tunable control parameters of input power and shear flow drive.

In ref. [7] the following reduced dynamical model for confinement transitions was derived from averaged energy moments of reduced MHD pressure and momentum convec-

978-1-4244-3872-3/09/$25.00 ©2009 IEEE

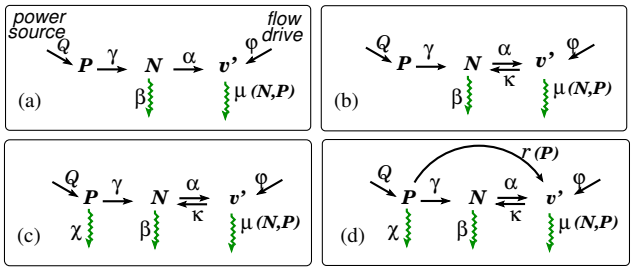

Fig. 1. Energy flux schematics for the gradient-driven plasma turbulence–shear flow system. Curly arrows indicate dissipative channels, straight arrows indicate inputs and transfer channels between the energy-containing subsystems. See text for explanations of each subfigure. (a) Energy fluxes modelled by Eqs 1–3; (b) energy fluxes modelled by Eqs 1, 4, and 5; (c) energy fluxes modelled by Eqs 4, 5, and 6; (d) energy fluxes modelled by Eqs 4, 7, and 8

.

tion equations in slab geometry:

$$\varepsilon \frac{dP}{dt} = Q - \gamma NP \tag{1}$$

$$\frac{dN}{dt} = \gamma NP - \alpha v'^2 N - \beta N^2 \tag{2}$$

$$2\frac{dv'}{dt} = \alpha v' N - \mu(P,N)v' + \varphi, \tag{3}$$

where P is the pressure gradient potential energy, N is the kinetic energy of the turbulence, and $F = \pm v'^2$ is the shear flow kinetic energy. The power input Q is assumed constant, ε is the thermal capacitance, γ and α are conservative energy transfer rate coefficients, β is the turbulence dissipation rate coefficient, φ is a shear flow source rate, and $\mu(P,N) = bP^{-3/2} + aPN$ represents the neoclassical and turbulent contributions to viscous dissipation. It is helpful to schematize the energy pathways through the P, N, and F subsystems as in Fig. 1. The skeleton of this dynamical system can be written down directly from (a) by inspection and fleshed out by using specific rate expressions, which were derived in [8] and [7] from semi-empirical arguments or given as ansatzes.

The bifurcation structure of Eqs 1–3 predicts shear flow suppression of turbulence, hysteretic, non-hysteretic, and oscillatory transitions, and saturation then decrease of the shear flow with power input due to pressure-dependent anomalous viscosity. All of these behaviors have been observed consistently in magnetically contained fusion plasma systems [2]. The model would therefore seem to be a "good" and "complete" one, in the sense of being self-consistent, free of pathological or persistent degenerate singularities, and reflecting typical observed behaviors.

However, there are several outstanding issues that suggest the model is still incomplete. The first issue arises as a gremlin in the bifurcation structure of Eqs 1–3 that makes a non-physical prediction. In section II a critical review of the bifurcation structure brings to light the previously unrecognized problem of trapped degenerate singularities. This leads in to section III, where a trapped singularity is unfolded smoothly by introducing another layer that models the previously neglected physics of downscale energy transfer. The second issue comes from a thermal diffusivity term that was regarded as negligible in the previous work. Section IV follows the qualitative changes to the bifurcation and stability structure that are due to potential energy diffusivity losses. The third issue arises from the two strands in literature on the physics of confinement transitions. In section V the unified model is proposed, in which is included a direct channel between gradient potential energy and shear flow kinetic energy. The results and conclusions are summarized in section VI.

A systematic and very practical methodology for characterizing the equilibria of dynamical systems involves locating and classifying high-order singularities then perturbing around them to explore and map the bifurcation landscape [9]. In a broad sense this paper is about applying singularity theory as a diagnostic tool while an impasto picture of confinement transition dynamics is compounded. The objective is to probe the relationship between the bifurcation and stability properties of the model and the physics of the system it is supposed to represent. In doing so, we shall take a guided walking tour of Eqs 1–3 and modifications and extensions to this system to study the type, multiplicity, and stability of attractors, interrogate degenerate or pathological singularities where they appear, and classify and map the bifurcation structure. The guiding motif is understanding the qualitative structure and properties of the system rather than concern for verisimilitude.

II. Symmetry-breaking has both local and global consequences

A bifurcation diagram for Eqs 1–3 is given in Fig. 2(a), where the power input Q is chosen as the principal bifurcation or control parameter. (In these and subsequent diagrams solid lines mark stable equilibria, dashed lines mark unstable equilibria, and amplitude envelopes of limit cycles are indicated by solid dots.) It is rich with information that speaks of the known and predicted dynamics of the system and foretells ways in which the model can be improved further. Two features in particular are to be noted:

(1) The system may be evolved to an equilibrium on the antisymmetric, $-v'$ branch, but if the power input then ebbs below the turning point at $(v', Q) \approx (-0.9, 0.46)$ the shear flow must *spontaneously* reverse direction, nominally to the lower $+v'$ branch. The zoom-in shows an example of an unusual feature in a bifurcation landscape, a region where there is fivefold multiplicity comprising three stable and two unstable equilibria. Two other, quite different, examples of threefold stable domains will be shown in section IV. In the remainder of this paper I concentrate on the $+v'$ branch and ignore the $-v'$ regime.

(2) For $\varphi = 0$ the bifurcation diagram features a symmetric pitchfork at $v' = 0$, thus φ is a local symmetry-breaking parameter. However φ **has more far-reaching effects than merely providing a local universal unfolding of the pitchfork**, for the branch of *unstable* equilibrium solutions that is just evident in the top (lower) left-hand corner was

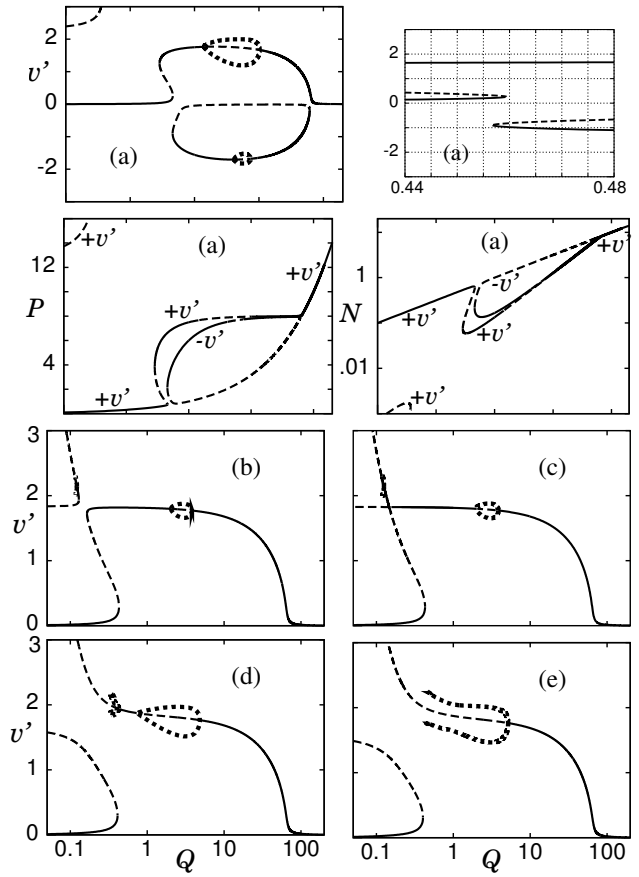

Fig. 2. Steady state and periodic solutions of Eqs 1–3 as a function of the power input Q. (a) $\varphi = 0.05$, $\varepsilon = 1.5$. The solution curves in the N and P diagrams are annotated to indicate whether they correspond to the $+v'$ or $-v'$ domain. (b)–(e) $\varepsilon = 1$. (b) $\varphi = 0.08$, (c) $\varphi \approx 0.08059 = \varphi_{Tm}$, (d) $\varphi = 0.1$, (e) $\varphi = 0.11$. Other parameters: $\beta = 1$, $\gamma = 1$, $b = 1$, $a = 0.3$, $\alpha = 2.4$.

trapped as a singularity at $(v', Q) = (\infty, 0)$ for $\varphi = 0$. As φ is increased this "new" branch passes through the heart of the model, the organizing centre. In (b) a segment of stable solutions has been created on the "new" branch as the Hopf bifurcation, which was born through a double zero eigenvalue (DZE), moves away from the turning point; the small branch of limit cycles can also be seen. At φ_{Tm} — the organizing centre — the "new" and "old" branches exchange arms, (c), via an unusual, non-symmetric, transcritical bifurcation. This point signals a profound change in the *type* of dynamics that the system is capable of. For $\varphi > \varphi_{TM}$, (d) and (e), a transition must still occur at the lower turning point, but classical hysteresis is (locally) forbidden.

III. Shear flows also generate turbulence

The first issue of incompleteness germinates from a pathology in the bifurcation structure of the model, which implies infinite growth of shear flow as the power input *falls*. Before we pinpoint the culprit singularity, it is illuminating to evince the physical — or non-physical — situation by considering Eqs 1–3 on the stretched (or shrunken) timescale $\tau = t/\varepsilon$. In a system of low thermal capacitance $\varepsilon \ll 1$ and $N \approx N_0$ and $v' \approx v_0$. Thus the dynamics becomes quasi one-dimensional: the potential energy subsystem sees the kinetic energy subsystems as nearly constant, and $P \approx (P_0 - Q/(N_0\gamma))\exp(-N_0\gamma\tau) + Q/(N_0\gamma)$. Reverting to real time, as $\varepsilon dP/dt \to 0$ we have $P \approx Q/(\gamma N)$; the potential energy is reciprocally slaved to the kinetic energy dynamics. The anomaly in this low-capacitance picture is that, as the power input Q ebbs toward zero, the shear flow can grow quite unrealistically. In Fig. 2(e) the conjectured fate of the surviving Hopf bifurcation is a double zero eigenvalue trap at $(Q, v') = (0, \infty)$. Numerical experiments show that with diminishing ε the Hopf bifurcation moves upwards along the curve, the branch of limit cycles shrinks, and the conjugate pair of pure imaginary eigenvalues approaches zero. It would seem, therefore, that some important physics is still missing from the model.

A. A trapped singularity is found and released

What is not shown in Fig. 2 (because a log scale is used for illustrative purposes) is a highly degenerate branch of equilibria that exists at $Q = 0$ where $N = 0$ and $v' = (P^{3/2}\varphi)/b$; it is shown in Fig. 3(a). For $\varphi > 0$ there is a trapped degenerate turning point, annotated as s4, where the "new" branch crosses the $Q = 0$ branch. (In this and subsequent diagrams, where amplitude envelopes of oscillatory domains are not plotted for clarity, the Hopf bifurcations are annotated with asterisks.)

The key to the release (or unfolding) of s4 lies in recognising that kinetic energy in large-scale structures inevitably feeds the growth of turbulence at smaller scales, as well as vice versa [2]. In a flow where fluid elements locally experience a velocity field that is strongly two-dimensional there will be a strong tendency to upscale energy transfer (or inverse energy cascade, see [1]), but the net rate of energy transfer to high wavenumbers (or Kolmogorov

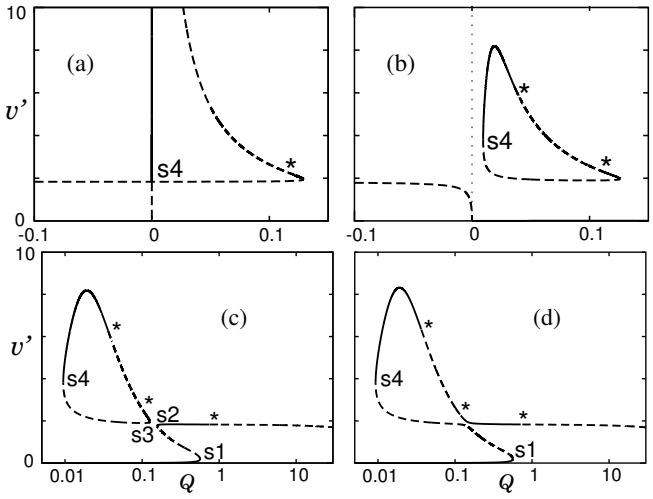

Fig. 3. Steady state and periodic solutions of Eqs 1, 4, and 5 as a function of the power input Q.(a) $\kappa = 0$, $\varphi = 0.08$; (b) $\kappa = 0.001$, $\varphi = 0.08$; (c) $\kappa = 0.001$, $\varphi = 0.083$; (d) $\kappa = 0.001$, $\varphi = 0.084$. Other parameters: $b = 1$, $\gamma = 1$, $\varepsilon = 1$, $\beta = 0.3$, $a = 0.3$, $\alpha = 2.4$.

cascade, see [10]) is not negligible. What amounts to an ultraviolet catastrophe in the physics when energy transfer to high wavenumbers is neglected maps to a trapped degenerate singularity in the mathematical structure of the model. The trapped singularity s4 may be unfolded smoothly by including a simple, conservative, back-transfer rate between the shear flow and turbulence subsystems:

$$\frac{dN}{dt} = \gamma NP - \alpha v'^2 N - \beta N^2 + \kappa v'^2 \quad (4)$$

$$2\frac{dv'}{dt} = \alpha v' N - \mu(P,N)v' + \varphi - \kappa v'. \quad (5)$$

The enhanced model consists of Eqs 1, 4, and 5, and the corresponding energy flux diagram is Fig. 1(b). The back-transfer rate coefficient κ need not be identified with any particular animal in the zoo of plasma and fluid instabilities, such as the Kelvin-Helmholtz instability; at this level it is simply a lumped dimensionless parameter that expresses the inevitability of energy transfer to high wavenumbers. The stability structure of this enhanced model was investigated in [11].

The manner and consequences of unfolding s4 can be appreciated from Fig. 3b, from which one learns a salutary lesson: non-physical equilibria and singularities should not be ignored or dismissed as irrelevant, because they can play an important role in determining bifurcation structure in the physical domain.

The unfolding creates a maximum in the shear flow, and (apparently) a *fourth* Hopf bifurcation is released from a trap at infinity. At the given values of the other parameters a finite-area isola of steady-state solutions is formed, but it is important to visualize this (or, indeed, any other) bifurcation diagram as a slice of a three-dimensional surface of equilibrium solutions, where the third coordinate is another parameter. (Isolas of steady-state solutions were first reported in the chemical engineering literature, where dynamical models typically include a thermal or chemical autocatalytic reaction rate [12].) Figure 3(c) and (d) show two slices of this surface, taken to demonstrate that the organizing centre is preserved through the unfolding of s4. Here the other turning points are labelled s1, s2, and s3. Walking through (c) and (d) we make the forward transition at s1 and progress along this branch through the onset of a limit cycle régime, as in Fig. 2. For obvious reasons this segment is now designated as the *intermediate* shear flow branch, and the isola or peninsula as the *high* shear flow branch. In (c) a back-transition occurs at s2. The system can only reach a stable attractor on the isola via a transient, either a non-quasistatic jump in a second parameter or an evolution from initial conditions within the appropriate basin of attraction. In (d) as we make our quasistatic way along the intermediate branch with diminishing Q the shear flow begins to grow, then passes through a second oscillatory domain before reaching a maximum and dropping steeply; the back transition in this case occurs at s4.

To reiterate this last point: the shear flow can actually grow as the power input is withdrawn. This is an important and testable prediction.

IV. Thermal dissipation affects the bifurcation structure

In the model so far the only outlet channel for the potential energy is conversion to turbulent kinetic energy, given by the conservative transfer rate γPN. However, in a driven dissipative system such as a plasma other conduits for gradient potential energy may be significant. The cross-field thermal diffusivity, a neoclassical transport quantity [13] is often assumed to be negligible in the strongly-driven turbulent milieu of a tokamak plasma [14], [8], [7], but here Eq. 1 is modified to include explicitly a linear "infinite sink" thermal energy dissipation rate:

$$\varepsilon\frac{dP}{dt} = Q - \gamma NP - \chi P. \quad (6)$$

Following ref. [15] χ is taken as a lumped dimensionless parameter and the rate term χP as representing all non-turbulent or residual losses such as neoclassical and radiative losses. The model now consists of Eqs 4, 5, and 6.

In Fig. 4 a series of bifurcation diagrams has been computed for increasing values of χ and a connected slice of the steady state surface. The corresponding energy schematic is Fig. 1(c). A qualitative change is immediately apparent, which has profound and far-reaching consequences: for $\chi > 0$ the two new turning points s5 and s6 appear, born from a local cusp singularity. Overall, from (a) to (e) we see that s1 does not shift significantly but that the peninsula becomes more tilted and shifts to higher Q, but let us begin a walking tour at s1 in (b). Here, as in Fig. 3, the transition occurs to an intermediate shear-flow state and further increments of Q take the system through an oscillatory régime. But the effect of *decreasing* Q is radically different: at s6 a discontinuous transition occurs to a high shear flow state on the stable segment of the peninsula. From this point we may step forward through the shear flow maximum and fall back to the intermediate branch at s5. We see that over the range of Q between s5 and s6 the system has five steady states, comprising three stable interleaved with two unstable steady states. As in Fig. 3(c) and (d) a back transition at low Q occurs at s4.

The tri-stable régime in (b) has disappeared in (c) in a surprisingly mundane way: not through a singularity but merely by a shift of the peninsula toward higher Q. But this shift induces a *different* tristable régime through the creation of s7 and s8 at another local cusp singularity. In (d) s4 and s7 have been annihilated at yet another local cusp singularity. It is interesting and quite amusing to puzzle over the 2-parameter lines of s1, s4, s5, s6, s7, and s8 over χ projected in Fig. 5. The origins of the four cusps can be read off the diagram, keeping in mind that the crossovers are a *trompe de l'oeil*: they are non-local. Since the two black areas do not overlap, there is no domain of sevenfold multiplicity in the system!

Returning to Fig. 4, at s5 in (c), (d), and (e) the system transits to a limit cycle, rather than to a stable intermedi-

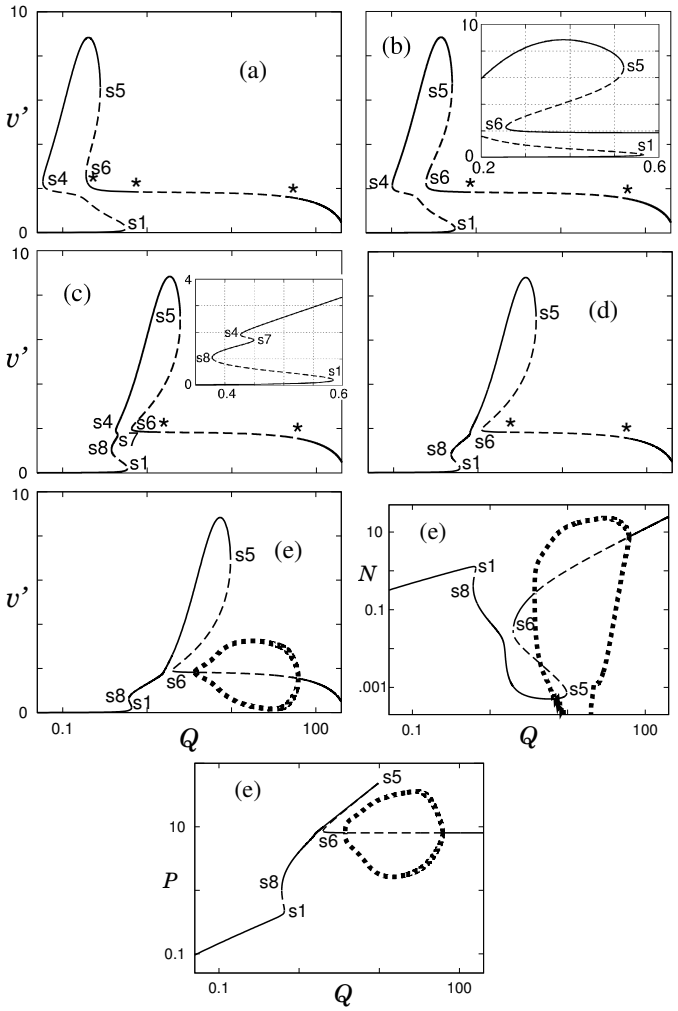

Fig. 4. Steady state and periodic solutions of Eqs 4, 5, and 6 as a function of the power input Q.(a) $\chi = 0.005$, (b) $\chi = 0.01$, (c) $\chi = 0.05$, (d) $\chi = 0.1$, (e) $\chi = 0.2$. $\kappa = 0.001$, $\varphi = 0.088$, $\beta = 0.3$, $b = 1$, $a = 0.3$, $\alpha = 2.4$, $\gamma = 1$, $\varepsilon = 1$.

ate steady state. The amplitude envelope of the oscillatory règime is included in (e), and shown are the bifurcation diagrams in N and P as well as v'. The turbulence is enormously suppressed due to uptake of energy by the shear flow, but rises again dramatically with this hard onset of oscillations. The pressure gradient jumps at s1 because the power input exceeds the distribution rates, and oscillatory dynamics between the energy subsystems sets in abruptly at s5.

V. A UNIFIED MODEL INCLUDES A NONLINEAR SHEAR FLOW DRIVE

In section I the two major strands of investigation into the physics of L–H transitions were described, and the models analysed in sections II–IV are limited to strand I physics where the transitions are an internal, quasi two-dimensional flow phenomenon. In this section I extend the models to include strand II physics self-consistently. In strand (II) in the literature confinement transitions are modelled in terms

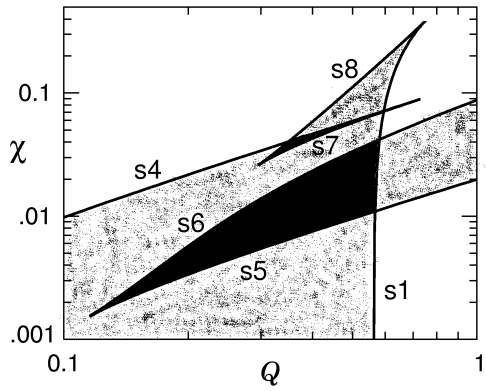

Fig. 5. In the two black areas there are five steady states and in the dusted areas there are three steady states.

of a nonlinear electric field driving torque created by nonambipolar ion orbit losses from the plasma edge region [4], [5], [6]. Although there are many supporting experiments [16], the "electric field bifurcation" model cannot explain shear flow suppression of turbulence, because it has no coupling to the internal dynamics of energy transfers from the potential energy reservoir. Here this plasma edge physics is treated as a piece of a more holistic picture and a simple rate $r(P)$ of shear flow generation due to ion orbit losses is used to complete the model, which now consists of Eq. 4 and

$$\varepsilon \frac{dP}{dt} = Q - \gamma NP - v'^2 r(P) - \chi P \tag{7}$$

$$2\frac{dv'}{dt} = \alpha v' N - \mu(P,N)v' + v' r(P) - \kappa v' + \varphi, \tag{8}$$

where, following the earlier authors, $r(P) = \nu \exp\left[-\left(w^2/P\right)^2\right]$. This expression simply says that the rate at which ions are preferentially lost, and hence flow is generated, is proportional to a collision frequency ν times the fraction of those collisions that result in ions with sufficient energy to escape. The form of the energy factor assumes an ion distribution that is approximately Maxwellian and w^2, analogous to an activation energy, is proportional to the square of the critical escape velocity. In this form of the rate expression I have explicitly included the temperature-dependence of r, through P, which couples it to the rest of the system. If w is high the rate is highly temperature (pressure gradient) sensitive. (For heuristic purposes constant density is assumed, constants and numerical factors are normalized to 1, and the relatively weak temperature dependence of the collision rate ν is ignored.) The corresponding energy schematic is Fig. 1(d) where it is seen that $r(P)$ is a competing potential energy conversion channel, that can dominate the dynamics when the critical escape velocity w is low or the pressure is high.

This is exactly what we see in the bifurcation diagrams, Fig. 6. Overall, the effect of this contribution to shear flow generation from the ion orbit loss torque is to elongate and flatten the high shear flow peninsula. The Hopf bifurcations that are starred in (a), where the contribution is relatively

small, have disappeared in (b) at a DZE singularity. What this means is that as $r(P)$ begins to take over there is no longer a practicably accessible intermediate branch in the transition region, because the intermediate branch is unstable until the remaining Hopf bifurcation is encountered at extremely high Q. Locally, in the transition region, the bifurcation diagram begins to look more like the simple S-shaped, cubic normal form schematics with classical hysteresis featured in numerous papers by earlier authors (e.g., [4]). However, as can be seen in Fig. 6(b) where the bifurcation diagram is rendered in the turbulent kinetic energy N, this **unified** model accounts for shear flow suppression of the turbulence, whereas theirs could not.

VI. Summary and conclusions

The generation of stable shear flows and associated confinement transitions and oscillatory behavior in magnetic fusion plasmas is regulated by Reynolds stress decorrelation of gradient-driven turbulence and/or by an induced bistable radial electric field. These two mechanisms are seamlessly unified by a smooth path through the singularity and bifurcation structure of a reduced dynamical model for this system.

The model is constructed self-consistently, beginning from simple rate-laws derived from the basic pathways for energy transfer from pressure gradient to shear flows. It is iteratively strengthened by finding and classifying the singularities and allowing them to "speak for themselves", then matching up appropriate physics to their unfoldings. The smooth path from turbulence driven to electric field driven shear flows crosses an interesting landscape:

- Hysteresis is possible in both régimes and is governed by different physics.
- A metamorphosis of the dynamics is encountered, near which hysteretic transitions are forbidden. The metamorphosis is a robust organizing centre of codimension 1, even though there are singularities of higher codimension in the system.
- Transitions may occur to and from oscillatory states.
- To traverse the smooth path several obstacles are successively negotiated in physically meaningful ways: a pitchfork is dissolved, which non-locally releases a branch of solutions from a trap at infinity, a singularity is released from a trap at zero power input, and two régimes of fivefold multiplicity are reconnoitred.

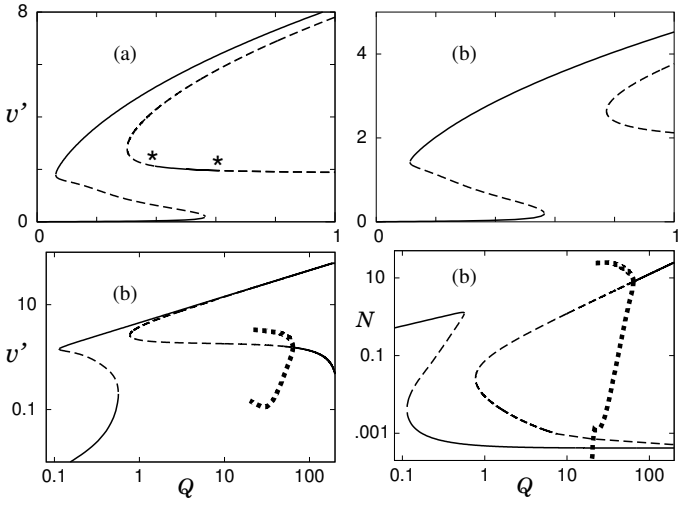

Fig. 6. Steady state and periodic solutions of Eqs 4, 7, and 8 as a function of the power input Q. (a) $\nu = 0.015$, (b) $\nu = 0.05$. $\chi = 0.01$, $\kappa = 0.001$, $\varphi = 0.088$, $\beta = 0.3$, $a = 0.3$, $\alpha = 2.4$, $b = \gamma = \varepsilon = w = 1$.

These results suggest strategies for controlling access to high confinement states, reducing turbulent transport, and manipulating oscillatory behaviour in new-generation fusion experiments that aim to achieve a self-sustaining burning plasma. More generally I have shown that low-dimensional models have a useful role to play in the study of one of the most formidable of complex systems, a strongly driven turbulent plasma.

References

[1] R. H. Kraichnan and D. Montgomery, "Two-dimensional turbulence," *Reports on Progress in Physics*, vol. 43, pp. 547–619, 1980.

[2] P. W. Terry, "Suppression of turbulence and transport by sheared flow," *Reviews of Modern Physics*, vol. 72, no. 1, pp. 109–165, 2000.

[3] P. H. Diamond, V. Shapiro, V. Shevchenko, Y. B. Kim, M. N. Rosenbluth, B. A. Carreras, K. Sidikman, V. E. Lynch, L. Garcia, P. W. Terry, and R. Z. Sagdeev, "Self-regulated shear flow turbulence in confined plasmas: basic concepts and potential applications to the L→H transition," *Proc. 14th International Conference on Plasma Phys. and Control. Nucl. Fus. Res.*, vol. 2, pp. 97–113, 1992.

[4] S.-I. Itoh and K. Itoh, "Model of *L*- to *H*-mode transition in tokamak," *Phys. Rev. Lett.*, vol. 60, no. 22, pp. 2276–2279, 1988.

[5] K.C. Shaing and E.C. Jr Crume, "Bifurcation theory of poloidal rotation in tokamaks: a model for the L–H transition," *Phys. Rev. Lett.*, vol. 63, no. 21, pp. 2369–2372, 1989.

[6] T. E. Stringer, "Explanation of the L–H mode transition induced by applied voltage," *Nuclear Fusion*, vol. 33, no. 9, pp. 1249–1265, 1993.

[7] R. Ball, R. L. Dewar, and H. Sugama, "Metamorphosis of plasma shear flow–turbulence dynamics through a transcritical bifurcation," *Phys. Rev. E*, vol. 66, pp. 066408–1–066408–9, 2002.

[8] H. Sugama and W. Horton, "L–H confinement mode dynamics in three-dimensional state space," *Plasma Phys. Control. Fusion*, vol. 37, pp. 345–362, 1995.

[9] M. Golubitsky and D. G. Schaeffer, *Singularities and Groups in Bifurcation Theory*, vol. 1, Springer–Verlag, New York, 1985.

[10] R. Ball, "The Kolmogorov cascade," in *Encyclopedia of Nolinear Science*, Alwyn Scott, Ed. 2004, Routledge.

[11] R. Ball, "Suppression of turbulence at low power input in a model for plasma confinement transitions," *Physics of Plasmas*, vol. 12, pp. 090904-1–8, 2005.

[12] R. Ball, "The origins and limits of thermal steady state multiplicity in the continuous stirred tank reactor," *Proc. R. Soc. Lond. A*, vol. 455, pp. 141–161, 1999.

[13] S. I. Braginskii, "Transport processes in a plasma," in *Reviews of Plasma Physics*, M. A. Leontovich, Ed., vol. 1. Consultants Bureau, New York, 1965.

[14] H. Sugama and W. Horton, "Shear flow generation by Reynolds stress and suppression of resistive g modes," *Phys. Plasmas*, vol. 1, no. 2, pp. 345–355, 1994.

[15] A. Thyagaraja, F. A. Haas, and D. J. Harvey, "A nonlinear dynamical model of relaxation oscillations in tokamaks," *Physics of Plasmas*, vol. 6, no. 6, pp. 2380–2392, 1999.

[16] A. Fujisawa, "Experimental studies of structural bifurcation in stellarator plasmas," *Plasma Phys. Control. Fusion*, vol. 45, pp. R1–AR88, 2003.

Acknowledgment

This work is supported by the Australian Research Council.